Optics Letters

Seeded optical parametric oscillator light source for precision spectroscopy

Z.-T. Zhang,[1] Y. Tan,[1,2] J. Wang,[1,2] C.-F. Cheng,[1,2,*] Y. R. Sun,[1,2] A.-W. Liu,[1,2] and S.-M. Hu[1,2,3]

[1]Hefei National Laboratory for Physical Sciences at Microscale, iChem Center, University of Science and Technology of China, Hefei 230026, China
[2]CAS Center for Excellence in Quantum Information and Quantum Physics, University of Science and Technology of China, Hefei 230026, China
[3]e-mail: smhu@ustc.edu.cn
*Corresponding author: cfcheng@ustc.edu.cn

Received 29 November 2019; revised 26 December 2019; accepted 26 December 2019; posted 3 January 2020 (Doc. ID 384582); published 14 February 2020

Precision spectroscopy of fundamental bands of molecules in the mid-infrared (MIR) region is of great interest in applications of trace detection and testing fundamental physics, where high-power and narrow-linewidth MIR lasers are needed. By using a frequency-stabilized near-infrared laser as a seed of the signal light of a continuous-wave optical parametric oscillator, we established a broadly tunable MIR light source that has an output power of several hundred milliwatts and a linewidth of a few tens of kilohertz. The MIR laser frequency drift was reduced to below 1 kHz by using an optical frequency comb to stabilize the frequency of the 1064 nm pumping laser. The performance of the light source was investigated and tested by measuring the saturated absorption spectroscopy of a few molecular transitions at 3.3 μm.

https://doi.org/10.1364/OL.384582

Owing to the increasing precision, spectroscopic methods have long been employed in testing fundamental physics and in search of new physics [1,2]. Essentially the goal could be accomplished by the determination of transition frequencies or minute frequency shifts in a quantum system. The development of precision spectroscopy techniques in the last two decades, including optical frequency combs (OFCs) and ultrastable lasers, has led to great success in applications of precision measurements in atomic systems [3–6].

Various laser absorption spectroscopy methods have been applied in fundamental studies of molecules [2,7–9], as well as in fast and non-intrusive trace gas analysis [10–12]. In the mid-infrared (MIR) region, many molecules have strong fundamental vibrational transitions, which are particularly suitable for related applications. Highly sensitive MIR spectroscopy enables the detection and quantitative analysis of trace gases in a variety of physical, chemical, biological, and industrial processes. Due to further improvements in sensitivity, MIR laser spectroscopy can be combined with other techniques such as molecular beam and ion detection, which are of great importance for precision measurements.

However, MIR precision spectroscopy has some inconveniences in terms of the light source and frequency calibration compared to near-IR (NIR) spectroscopy. In the past few decades, various continuous-wave (CW) MIR sources have been developed. Some gas lasers have relatively high output power and ultra-narrow linewidths, which are very useful for precision measurements [13,14] but are available around only a few wavelengths. The development of quantum well engineering technology has led to wide use of commercial quantum cascade lasers (QCLs) [15,16], but their high-precision frequency calibration needs MIR frequency combs [17] that are not yet mature, or up-conversion to the NIR region where commercial OFCs are available. The technology of periodically polarized crystals, especially periodically poled lithium niobate (PPLN) crystals, has driven the widespread use of differential frequency generation (DFG) [18,19] and high-efficiency CW optical parametric oscillators (OPOs) [20–22], which have a broad tuning range and can be easily calibrated by NIR frequency combs. Nevertheless, how to realize sufficient output power and accurate control of the wavelength at the same time is still a challenge in MIR precision spectroscopy.

Here, we report a seeded singly resonant CW-OPO system with a MIR output power of several hundred milliwatts and a spectral linewidth of less than 20 kHz. A narrow-linewidth laser beam was injected into the OPO cavity as a seed of the NIR signal light, which resulted in a reduced linewidth of the idler light emission in the MIR region. By locking the pump and seed light to a NIR frequency comb, long-term stability was also maintained with a frequency drift below 1 kHz. As a test of the MIR laser source, we recorded the sub-Doppler saturation spectroscopy of a few rovibrational transitions of CH_4 and C_2H_4 at 3.3 μm. The observed lines showed sub-megahertz widths due mostly to the transit-time broadening, and their positions were determined with an accuracy of a few kilohertz. The method offers an excellent opportunity for precision measurements and other spectroscopy applications in the MIR region.

The scheme of the experimental setup is shown in Fig. 1. The configuration of the singly resonant OPO is similar to

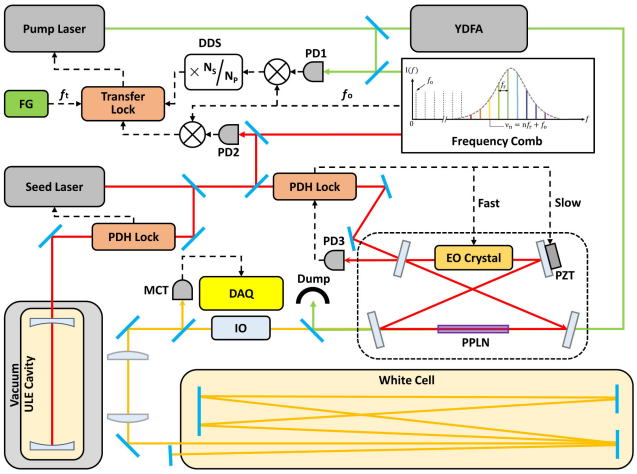

Fig. 1. Scheme of the experimental setup. Green, red, and yellow lines indicate pump light, seed/signal light, and idler light, respectively. YDFA, ytterbium-doped fiber amplifier; DDS, direct digital synthesizer; PD, photodiode detector; FG, function generator; PDH, Pound–Drever–Hall; EO crystal, electro-optical crystal; PZT, piezo actuator; DAQ, data acquisition system; MCT, mercury cadmium telluride detector; IO, optical isolator; ULE, ultra-low expansion cavity.

that reported in [23]. The pump light comes from a narrow-linewidth Nd:YAG laser (Mephisto S) and a Yb-doped fiber amplifier (YDFA) with an output power of up to 10 W at 1064 nm. The pump light is focused onto a 5 cm long MgO-doped multi-channel PPLN crystal placed inside the OPO cavity. The phase-matching wavelength ranges from 2.6 to 4.3 μm. The temperature of the crystal can be stabilized at a preset value between 40°C and 160°C with a precision of 0.002°C. The OPO cavity is a bow-tie ring cavity with four mirrors highly reflective (> 99.9%) at the signal wavelength of 1400–1800 nm and transparent at the pump and idler wavelengths. The idler light transmitted from the cavity is collimated and separated from the pump and signal laser beams by dichroic mirrors. The output MIR light beam, with a beam size of $\phi = 6$ mm, is attenuated and sent into a White-type multi-pass cell (optical path length 33 m) for Lamb-dip measurements.

A narrow-linewidth laser source is necessary to perform high-resolution spectroscopy. Moreover, the central frequency of the laser also needs to be stable enough during the period of the spectral scan, which typically takes several seconds or minutes. However, frequency jitters in conventional OPO light sources are usually at the level of 1 MHz due to vibration noise or temperature fluctuations. To reduce the linewidth and frequency drift of the idler light produced by our OPO system, we lock both frequencies of the pump and signal light. The details of locking are given as follows. A fiber laser (NKT Koheras AdjustiK E15, "Seed Laser" shown in Fig. 1) with a stated linewidth of 100 Hz (100 μs) at 1.57 μm is injected into the OPO cavity as a seed of the signal laser. The seed laser has been locked with a temperature-stabilized cavity made of ultra-low expansion (ULE) glass through a Pound-Drever-Hall (PDH) locking servo. The OPO cavity is locked to the injected seed light by another PDH locking servo. As shown in Fig. 1, the cavity-locking control signal is divided into a fast component and a slow component; the fast one with a bandwidth of about 5 MHz is applied on a homemade electro-optical phase modulator placed inside the OPO cavity, and the slow one is applied on a piezo actuator (PZT) attached to a cavity mirror. The fast feedback loop guarantees that the signal light keeps following with the seed light, while the slow feedback loop compensates for the long-term drift of the OPO cavity.

The pump laser has a manufacturer-specified linewidth of 5 kHz in 100 ms, and it is locked (feedback bandwidth 16 kHz) to the seed light by the transfer lock technique [24]. A frequency comb synthesized by an Er:fiber oscillator is used to link the pump laser and seed laser at different wavelengths. The transfer locking scheme allows us to cancel the noise of the frequency comb and gives a direct beat signal between these two lasers. As illustrated in Fig. 1, the beat frequency is locked at a preset frequency f_t by the transfer locking servo:

$$f_t = \frac{N_s}{N_p}(f_p - N_p f_r) - (f_s - N_s f_r) = \frac{N_s}{N_p} f_p - f_s, \quad \textbf{(1)}$$

where f_s is the frequency of the seed laser, which can be determined directly from its beat with the OFC, f_p is the frequency of the pump laser, and f_r is the repetition frequency of the frequency comb. N_p and N_s are integer numbers used in the direct digital synthesizer (DDS in Fig. 1), being equal to the comb tooth indices for the pump laser and the seed laser, respectively. In this way, we eliminate the noise in f_0, which is the carrier–envelope offset frequency, and f_r of the comb and lock the pump laser with the stabilized seed laser. Since both the signal light and pump light are locked and stabilized, the MIR idler light emitted from the OPO cavity is frequency stabilized, and its frequency can be tuned precisely by changing the frequency f_t applied in the transfer lock.

Without the injection of seeding light, the system is similar to a conventional OPO light source, and the lasing threshold was measured to be about 6.0 W. When we injected a seeding light into the OPO cavity, the character of the OPO emission changed dramatically. It was evidenced by the measurement of the power of the MIR emission from the cavity, as shown in Fig. 2. At a pumping power below 5 W, without injection of the seeding light, we could not observe any MIR emission from the cavity. When the seed laser was injected into the OPO cavity, we could observe considerable power of the MIR emission with a pumping power of 1–5 W, as shown in the inset in Fig. 2. The power of the injected seed light was measured to be about 150 mW before entering the cavity, and estimated to be about 10 W inside the cavity. Here the emission of the MIR light was likely from a differential frequency generation (DFG) process, but the efficiency was considerably higher than the conventional DFG system [25], and a clear nonlinear dependence on the input pumping power can be seen in Fig. 2. When the pumping power got higher than a threshold of about 5 W, a dramatic power increase of the MIR emission was observed. At a pumping power over 6 W, the MIR light power increased almost linearly to the pumping power, indicating that the OPO mechanism was taking the leading contribution.

Instead of measuring the linewidth of the MIR emission, we measured linewidths of the pumping laser and the signal light, both being in the NIR region. The beat signal between the signal light emitted from the OPO cavity and an independent narrow-linewidth fiber laser (NKT Koheras AdjustiK E15) was measured, and the result is shown in Fig. 3(a). In an averaging time of 1 s, the beat spectrum showed a linewidth [full

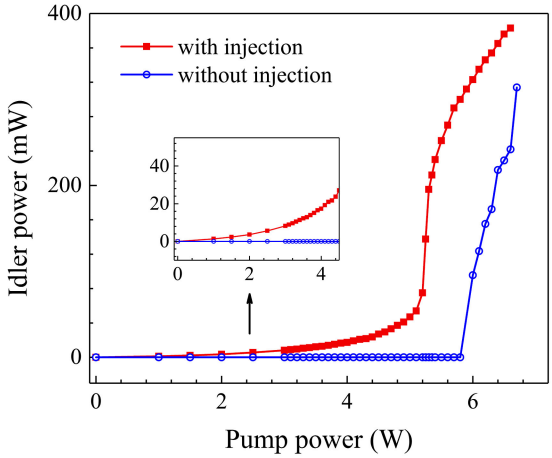

Fig. 2. Power of the MIR light obtained at a given pumping power. Red solid squares and blue hollow circles present results obtained with and without injection of the seed laser, respectively.

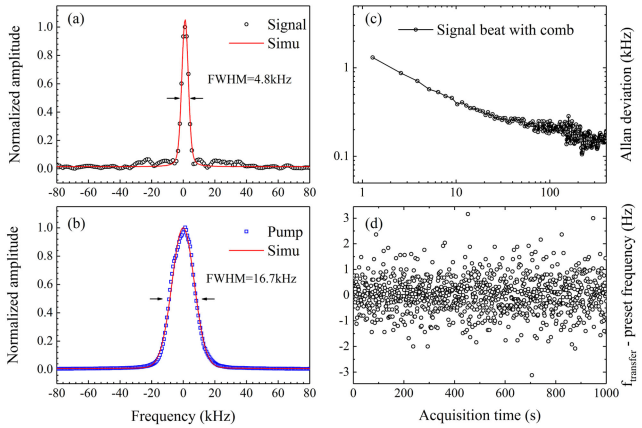

Fig. 3. Analysis of the short-term and long-term stability of the OPO emission. (a) Spectrum of the beat signal between the OPO signal light and an independent narrow-linewidth laser. (b) Spectrum of the beat signal between the OPO pump and seed light through an optical frequency comb. (c) Allan deviation of the beat frequency between the OPO signal light and an optical frequency comb. (d) Recorded transfer beat frequency between the OPO pump and seed light.

width at half maximum (FWHM)] of 4.8 kHz. Taking into account the resolution of the spectrum analyzer of 3 kHz, we can give an upper limit of the signal light linewidth as 3.7 kHz. The linewidth of the pump laser was measured by the transfer beating method [24] mentioned above. A spectrum of the beat signal recorded in an averaging time of 4.5 s is shown in Fig. 3(b), which has a linewidth of 16.7 kHz. Note that the actual linewidth could be narrower since the spectrum shown in Fig. 3(b) is a convolution of the laser spectrum, mechanical vibration noise from the environment, and various electric noises in the transfer beating measurement. Nevertheless, according to the spectra of the pumping laser and the signal light emitted from the OPO cavity, we can safely conclude that the linewidth of the MIR idler emission should be less than 20 kHz, being sufficiently narrow for precision spectroscopy measurement of molecules.

The absolute frequency of the MIR idler light was determined by measuring the frequencies of the NIR pumping laser and signal light by the OFC. Figure 3(c) shows the Allan deviation of the beating frequency between the signal light and the OFC. It indicates a long-term frequency stability better than a few hundred hertz, being limited by the rubidium clock that we used to lock the OFC. The pump laser was transfer-locked to the seed laser, and the transfer beat frequency recorded by a frequency counter is shown in Fig. 3(d). We can see that the frequency of the pump laser followed the seed laser quite well, and the frequency value can be derived according to Eq. (1).

As a demonstration of the seeded OPO system, saturated absorption spectra of two lines in the region of $3008.6 - 3013.7\ \mathrm{cm}^{-1}$ were recorded: one is the $13_{0,13} \leftarrow 12_{0,12}$ transition in the ν_{11} band of C_2H_4, and the other one is the P(1) line in the ν_3 band of CH_4. C_2H_4 and CH_4 samples were purchased from Nanjing Special Gas Factory with stated purity of 99.9% and purified by the "freeze-pump-thaw" method before use. About 25 mW of the MIR light was sent into a White-type multipass cell and retro-reflected to perform saturation spectroscopy. Taking into account the change in the beam diameter and power loss along the beam path, we estimated the effective saturation parameters as 0.3 and 0.2 for these two transitions, respectively. Spectroscopy measurements were performed at room temperature (296 K). Figure 4(a) shows a piece of the C_2H_4 spectrum recorded at a sample pressure of 0.49 Pa. Spectra were recorded at different sample pressures of 0.25 Pa, 0.49 Pa, 1.0 Pa, 1.6 Pa, and they were fitted using lorentzian profiles. A simulated spectrum is also shown as the red line in Fig. 4(a). The absolute transition frequency is determined to be 90,257,457.679(5) MHz, as a weighted average of the line centers obtained from spectra recorded at different pressures. This value agrees well with the result reported by Lebron and Tan [26] using Doppler-limited spectroscopy, while the accuracy has been improved by a factor of 3600. Figure 4(b) shows an example of the CH_4 spectrum recorded at a sample pressure of 0.52 Pa. The line center was determined to be 90,207,892.537(3) MHz, agreeing well with the value 90,207,892.542(2) MHz given by Abe *et al.* [27].

The width of the saturated absorption line was also derived from the fit of each spectrum. Figure 4(c) shows the C_2H_4 and CH_4 linewidths (FWHM) obtained at different sample pressures. A linear fit of the data yields a pressure-induced broadening coefficient of 239(14) kHz/Pa and a width of 433(17) kHz at the zero-pressure limit for C_2H_4, and the values for the CH_4 line are 191(24) kHz/Pa and 556(24) kHz, respectively. Various sources contribute to the linewidth at the zero-pressure limit, such as the natural linewidth of the transition, hyperfine splitting, transit-time broadening, imperfect counter-propagating light beams, laser linewidth, and power broadening. The natural linewidth and power broadening are negligible for both lines studied here. The broadening due to imperfect alignment should be below 3 kHz. The contribution from the hyperfine splitting should be less than 60 kHz for the CH_4 line [28] and is estimated to be similar for the C_2H_4 line. The main contribution should be the transit-time broadening at room temperature. Note that the non-planar wave of the laser beam due to concave mirrors (curvature radius of 1.5 m) installed in the White cell gives an additional broadening convoluted to the transit-time broadening. Using the formula given by Demtröder [29], the transit-time broadening

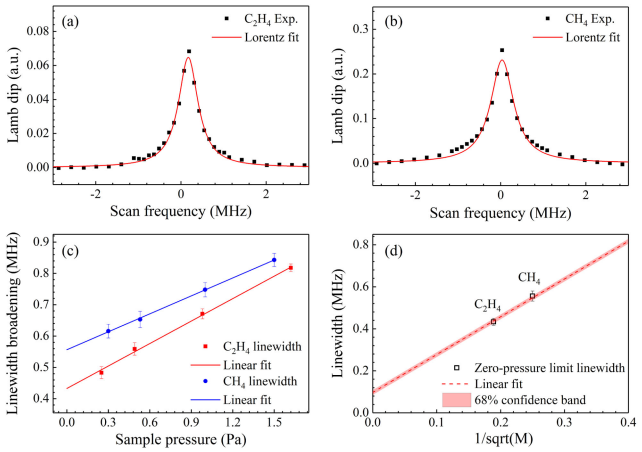

Fig. 4. Spectroscopy measurement using the mid-IR idler light produced by the seeded OPO system. (a) Saturated absorption spectrum of C_2H_4 at 3010.66 cm^{-1} with a sample pressure of 0.49 Pa. (b) Saturated absorption spectrum of CH_4 at 3009.01 cm^{-1} with a sample pressure of 0.52 Pa. (c) Lorentzian widths of the C_2H_4 (red square) and CH_4 (blue dotted) lines recorded at different sample pressures, respectively. (d) Lorentzian widths of the C_2H_4 and CH_4 lines at the zero-pressure limit versus the reversed square root of molecular molar mass $1/\sqrt{M}$.

is proportional to the mean speed of molecules. Consequently, we have $\gamma_t(M) = A/\sqrt{M}$, where M is the molar mass of the molecule, and the coefficient A can be calculated to be 1.80 MHz $(g/mol)^{1/2}$ according to our experimental conditions given above. As shown in Fig. 4(d), using a linear fit of the linewidths (at the zero-pressure limit) of C_2H_4 and CH_4 determined from our measurements, we derived $\gamma_0 = 97(14)$ kHz by fixing A at the calculated value. Since the width γ_0 includes contributions from the laser linewidth, hyperfine splitting, and other mass-independent and pressure-independent contributions, it indicates an upper limit of the MIR laser linewidth, consistent with the measurement shown in Fig. 3.

We developed a narrow-linewidth CW MIR light source based on a seeded OPO. A frequency-stabilized fiber laser was coupled into the OPO cavity as a seeding of the signal light. The pump laser was also stabilized with the seed laser by the transfer-lock technique using an OFC. The width of the MIR idler light emitted from the OPO cavity was examined by measuring the widths of the pump laser and signal light, respectively, at 17 kHz and 4 kHz. The long-term frequency drift was also determined to be below 1 kHz. As a demonstration, the light source was applied to measure the saturated absorption spectra of C_2H_4 and CH_4 rovibrational transitions at 3.3 μm. Lamb dips with sub-megahertz width were observed, and the line centers were determined with an accuracy of a few kilohertz. Such a high-power, frequency-stabilized, and widely tunable MIR light source meets the requirement of precision spectroscopy of molecules and can be used in some important applications, such as the Lamb-dip measurement of the hydrogen molecule for a test of quantum electrodynamics [8] and the optical detection of radioactive $^{14}CO_2$ [30,31].

Funding. National Natural Science Foundation of China (11974328, 21427804, 21688102); Chinese Academy of Sciences (XDB21020100).

Disclosures. The authors declare no conflicts of interest.

REFERENCES

1. M. S. Safronova, D. Budker, D. DeMille, D. F. J. Kimball, A. Derevianko, and C. W. Clark, Rev. Mod. Phys. **90**, 025008 (2018).
2. T. Steimle and W. Ubachs, J. Mol. Spectrosc. **300**, 1 (2014).
3. T. W. Hänsch, Rev. Mod. Phys. **78**, 1297 (2006).
4. C. W. Chou, D. B. Hume, T. Rosenband, and D. J. Wineland, Science **329**, 1630 (2010).
5. B. Spaun, P. B. Changala, D. Patterson, B. J. Bjork, O. H. Heckl, J. M. Doyle, and J. Ye, Nature **533**, 517 (2016).
6. A. Cingöz, D. C. Yost, T. K. Allison, A. Ruehl, M. E. Fermann, I. Hartl, and J. Ye, Nature **482**, 68 (2012).
7. C. F. Cheng, Y. R. Sun, H. Pan, J. Wang, A. W. Liu, A. Campargue, and S. M. Hu, Phys. Rev. A **85**, 024501 (2012).
8. L.-G. Tao, A.-W. Liu, K. Pachucki, J. Komasa, Y. R. Sun, J. Wang, and S.-M. Hu, Phys. Rev. Lett. **120**, 153001 (2018).
9. F. M. J. Cozijn, P. Dupré, E. J. Salumbides, K. S. E. Eikema, and W. Ubachs, Phys. Rev. Lett. **120**, 153002 (2018).
10. T. J. Kulp, S. E. Bisson, R. P. Bambha, T. A. Reichardt, U. B. Goers, K. W. Aniolek, D. A. V. Kliner, B. A. Richman, K. M. Armstrong, R. Sommers, R. Schmitt, P. E. Powers, O. Levi, T. Pinguet, M. Fejer, J. P. Koplow, L. Goldberg, and T. G. Mcrae, Appl. Phys. B **75**, 317 (2002).
11. M. M. J. W. van Herpen, S. Li, S. E. Bisson, S. Te Lintel Hekkert, and F. J. M. Harren, Appl. Phys. B **75**, 329 (2002).
12. F. Müller, A. Popp, F. Kühnemann, and S. Schiller, Opt. Exp. **11**, 2820 (2003).
13. A. Clairon, B. Dahmani, A. Filimon, and J. Rutman, IEEE Trans. Instrum Meas. **IM-34**, 265 (1985).
14. K. J. Siemsen, J. E. Bernard, A. A. Madej, and L. Marmet, Appl. Phys. B **72**, 567 (2001).
15. J. Faist, F. Capasso, D. L. Sivco, C. Sirtori, A. L. Hutchinson, and A. Y. Cho, Science **264**, 553 (1994).
16. M. Beck, D. Hofstetter, T. Aellen, J. Faist, U. Oesterle, M. Ilegems, E. Gini, and H. Melchior, Science **295**, 301 (2002).
17. A. Gambetta, E. Vicentini, N. Coluccelli, Y. Wang, T. Fernandez, P. Maddaloni, P. De Natale, A. Castrillo, L. Gianfrani, P. Laporta, and G. Galzerano, APL Photon. **3**, 046103 (2018).
18. D. Mazzotti, P. Cancio, G. Giusfredi, P. De Natale, and M. Prevedelli, Opt. Lett. **30**, 997 (2005).
19. K. Takahata, T. Kobayashi, H. Sasada, Y. Nakajima, H. Inaba, and F.-L. Hong, Phys. Rev. A **80**, 032518 (2009).
20. D. Chen, D. Hinkley, J. Pyo, J. Swenson, and R. Fields, J. Opt. Soc. Am. B **15**, 1693 (1998).
21. E. V. Kovalchuk, T. Schuldt, and A. Peters, Opt. Lett. **30**, 3141 (2005).
22. I. Ricciardi, E. De Tommasi, P. Maddaloni, S. Mosca, A. Rocco, J.-J. Zondy, M. De Rosa, and P. De Natale, Opt. Express **20**, 9178 (2012).
23. T.-H. My, C. Drag, and F. Bretenaker, Opt. Lett. **33**, 1455 (2008).
24. H. R. Telle, B. Lipphardt, and J. Stenger, Appl. Phys. B **74**, 1 (2002).
25. D. Richter, A. Fried, B. Wert, J. Walega, and F. Tittel, Appl. Phys. B **75**, 281 (2002).
26. G. Lebron and T. Tan, J. Mol. Spectrosc. **288**, 11 (2013).
27. M. Abe, K. Iwakuni, S. Okubo, and H. Sasada, J. Opt. Soc. Am. B **30**, 1027 (2013).
28. J. L. Hall and C. Bordé, Phys. Rev. Lett. **30**, 1101 (1973).
29. W. Demtröder, *Laser Spectroscopy Vol. 1: Basic Principles*, 4th ed. (Springer, 2008).
30. A. J. Fleisher, D. A. Long, Q. N. Liu, L. Gameson, and J. T. Hodges, J. Phys. Chem. Lett. **8**, 4550 (2017).
31. I. Galli, S. Bartalini, S. Borri, P. Cancio, D. Mazzotti, P. De Natale, and G. Giusfredi, Phys. Rev. Lett. **107**, 270802 (2011).